ISBN: 978-3-95450-227-1 ISSN: 2673-5490 doi:10.18429/JACoW-IPAC2022-TUPOST006

FREQUENCY-DEPENDENT RF VOLTAGE CALIBRATION USING LONGITUDINAL TOMOGRAPHY IN THE CERN PSB

D. Quartullo*, S. Albright, H. Damerau, CERN, Geneva, Switzerland

Abstract

Longitudinal phase-space tomography reconstructs the phase-space distribution from a set of bunch profiles and the accelerator parameters, which includes the RF voltage. The quality of the reconstruction depends on the accuracy to which these parameters are known. Therefore, it can be used for beam-based RF voltage calibration by analysing oscillations of a mismatched bunch. The actual RF voltage may be different from the programmed one due to uncertainties of the electrical gap voltage measurements and intensity effects. Tomography-based RF voltage calibration was systematically performed with low-intensity bunches in all four rings of the PS Booster (PSB) at injection and extraction energy. For each of the three RF cavities present in a given ring, the calibration was performed separately to extract the voltage errors while avoiding any influence of phase misalignments. The number of synchrotron oscillation periods available for the voltage calibration was constrained by the short duration of the PSB flat-bottom and top. Longitudinal beam dynamics simulations using the full PSB impedance model were performed to benchmark the results provided by the calibrations.

INTRODUCTION

Longitudinal tomography is a beam-based technique able to reconstruct the bunch distribution in longitudinal phase-space [1–4]. The main inputs are the measured bunch profiles, the output is the phase-space distribution whose projections best match the measured profiles. The discrepancy D represents the degree of matching between measured and reconstructed profiles. In a tomographic reconstruction, D typically decreases and reaches an asymptotic value $\widehat{D}$ after a sufficiently large number of iterations.

Tomography provides accurate results only when certain accelerator and beam parameters are known. While parameters like beam energy are normally known with high precision, the actual voltage V_d acting on the beam and the phase position $\widehat{\varphi}_\mathrm{s}$ of the bucket center with respect to the trigger are difficult to measure. In particular, V_d can be significantly different from the programmed voltage V_p, due to uncertainties in electrical voltage measurements and collective effects.

Tomography can be used to find V_d and $\widehat{\varphi}_\mathrm{s}$ [5–7] by determining the V_rf and φ_s values which minimize $\widehat{D}$. Two methods can be used, as shown in Fig.1. The first one computes $\widehat{D}$ for V_rf - φ_s pairs forming a rectangular grid to obtain the minimum $\widehat{D}$. The second method relies on a minimization algorithm which computes $\widehat{D}$ for selected V_rf - φ_s pairs and creates a path converging to the minimum $\widehat{D}$.

* danilo.quartullo@cern.ch

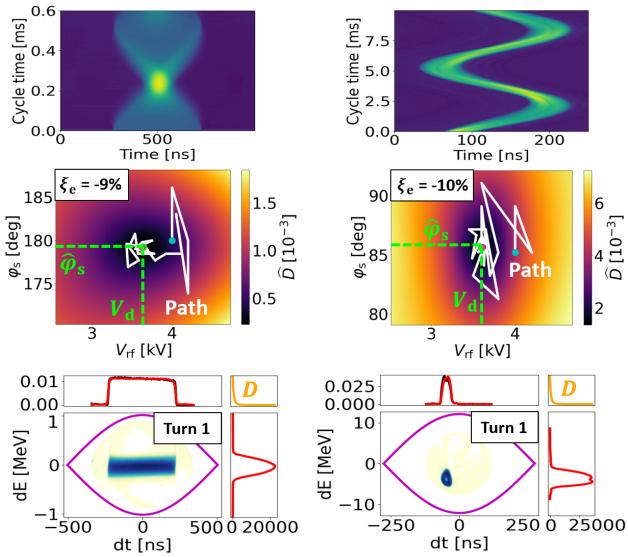

Figure 1: Top: bunch profiles measured with the S7 cavity at injection (left) and extraction (right) energy with V_p = 4 kV. Middle: voltage calibrations using as input the corresponding measured profiles shown above. Bottom: corresponding phase-space reconstructions at turn 1. The reconstructed (red) bunch profiles match well the measured (black) ones.

Bunch oscillations are needed for voltage calibration: if the bunch is perfectly matched, low discrepancy values are obtained with any voltage, since the longitudinal emittance is a free parameter.

The PSB consists of four superposed rings. Each ring is equipped with three independent RF cavities [8] in sectors 5 (S5), 7 (S7) and 13 (S13). In this contribution, tomography-based voltage calibration is applied to all the PSB RF cavities, at injection and extraction energies.

MEASUREMENTS SETUP

Beam measurements were performed at injection and extraction energies in each of the four PSB rings. The voltage at $h = 1$ in each of the cavities S5, S7 and S13 was measured separately in each ring for constant programmed voltages of 4 kV, 5 kV, 6 kV and 7.5 kV. For each combination of ring, cavity and programmed voltage, ten cycles were recorded. Low Level RF (LLRF) beam phase and radial loops were disabled to avoid damping bunch oscillations. The beam had low intensity to limit the influence of collective effects.

At flat-bottom, measurements started at injection and extended for the entire flat-bottom duration of 0.6 ms. At injection, the beam from Linac4 had a rectangular shape in the (dt, dE) phase space and was not matched to the RF

ISBN: 978-3-95450-227-1 ISSN: 2673-5490 doi:10.18429/JACoW-IPAC2022-TUPOST006

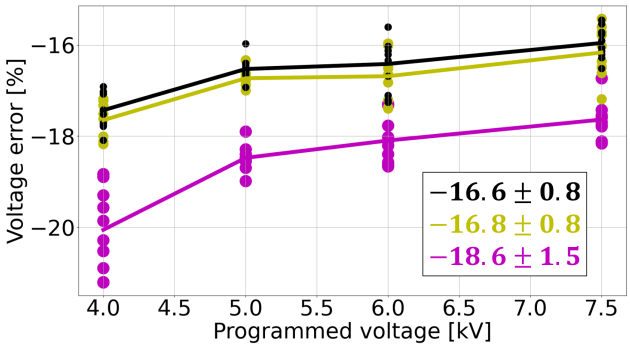

Figure 2: Voltage errors as a function of the programmed voltages for different numbers of synchrotron periods considered for voltage calibration: $N_{T_s} = 1$ (magenta), 1.5 (yellow) and 2.5 (black). Beam measurements were taken with the S13 cavity in ring 1 at extraction energy. For a given programmed voltage and N_{T_s}, the dots represent voltage errors for the ten measured accelerator cycles.

bucket, leading to strong quadrupole oscillations (Fig.1, top left). The bunch intensity, N_p, was below $8 \cdot 10^{10}$ p/b.

At extraction energy, measurements started at the beginning of the flat-top and extended for 10 ms. A larger time span could not be used due to the start of the extraction synchronization. Before the beginning of the flat-top, fast jumps of the programmed RF voltage enhanced quadrupole oscillations, while the transient when opening the phase loop created dipole oscillations (Fig.1, top right). The bunch intensity was below $3 \cdot 10^{10}$ p/b.

VOLTAGE CALIBRATION RESULTS

Voltage calibrations were performed with beam measurements recorded in early 2022. We studied how the relative voltage-error $\xi_e = (V_d - V_p)/V_p$ varied when the number N_{T_s} of synchrotron periods used for calibration was increased (Fig. 2). The measured time spans were sufficient to obtain convergence in all the cases, except for some cycles at flat-bottom with $V_p = 4$ kV. Convergence in ξ_e was reached for $N_{T_s} = 2.5$ and $N_{T_s} = 0.9$ at flat-top and bottom, respectively.

The voltage errors reported in Fig. 3 are those obtained at convergence. They vary between -7% and -20%, the S7 cavity provides the smallest voltage errors, whereas the S13 cavity gives the largest ξ_e, except in ring 2.

A cavity which provides lower ξ_e at flat-bottom also gives lower ξ_e at flat-top, indicating that the voltage errors are consistent amongst each other. For a given ring and cavity, ξ_e varies by maximum 3% going from flat-bottom to flat-top. Each group of ten measured cycles has usually a voltage-error spread within 1%, indicating an excellent reproducibility of results from cycle to cycle. The voltage-error spreads due to different V_p are below 3%.

The voltage errors at flat-bottom presented in Fig. 3 correspond well (within 4%) with voltage errors evaluated from beam measurements taken in 2021 (Fig. 4).

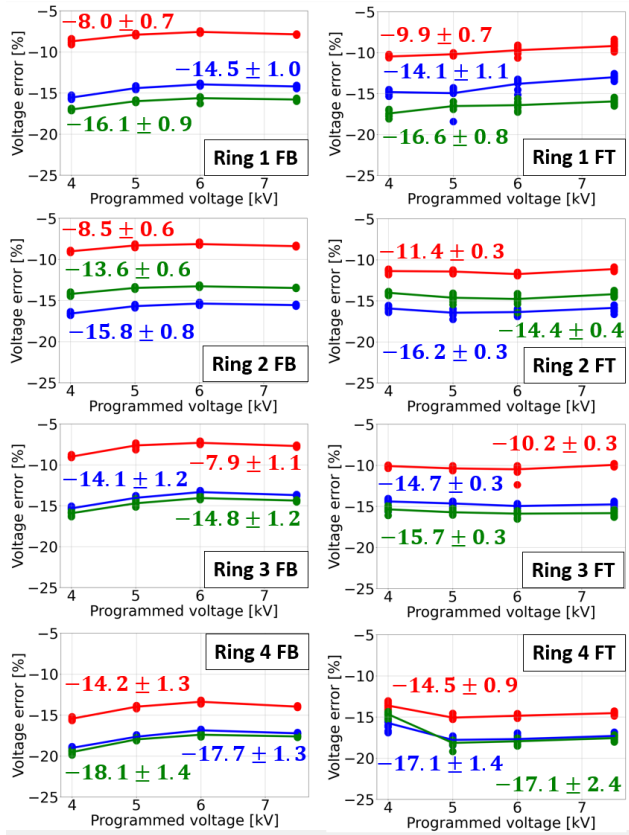

Figure 3: Voltage errors as a function of the programmed voltage for the S5 (blue), S7 (red) and S13 (green) cavities in each PSB ring at flat-bottom (left) and top (right). The beam measurements were taken in 2022. For a given beam energy, ring, cavity, and programmed voltage, the voltage errors for the ten measured acceleration cycles are represented by dots. In each plot, the voltage-error averages and spreads varying V_p are reported for the three cavities.

ESTIMATION OF SYNCHROTRON FREQUENCY RATIOS

As a cross-check that the obtained results were consistent amongst each other, we computed small-amplitude synchrotron frequency $f_{s,0}$ ratios either as square roots of voltage ratios or as ratios of synchrotron periods. The synchrotron periods were derived by examining the evolutions of bunch-profile positions and lengths, which were computed by using the Full Width at Half Maximum (FWHM).

As an example at flat-bottom, we considered two cycles with $V_p = 5$ kV (Fig. 5, top). The first cycle was measured in ring 4 with the S13 cavity, providing $\xi_e = -17.9\%$ and $V_d = 4.10$ kV, whereas the second cycle was measured in ring 1 with the S7 cavity, giving $\xi_e = -7.9\%$ and $V_d = 4.60$ kV. The $f_{s,0}$ ratio was 1.06 using V_d or synchrotron-period values, indicating an excellent agreement between the two methods.

At extraction energy, we examined two cycles with $V_p = 4$ kV (Fig. 5, bottom). The first cycle was measured in ring 1 with the S13 cavity, providing $V_d = 3.28$ kV, the

ISBN: 978-3-95450-227-1 ISSN: 2673-5490 doi:10.18429/JACoW-IPAC2022-TUPOST006

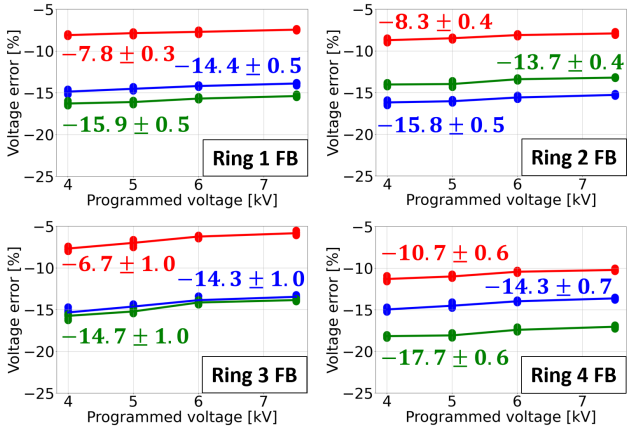

Figure 4: Voltage errors as a function of V_p for the S5 (blue), S7 (red) and S13 (green) cavities in each PSB ring at flat-bottom. The beam measurements were taken in 2021. For a given ring, cavity, and programmed voltage, the voltage errors for the ten measured acceleration cycles are represented by dots. Averages and spreads varying V_p are reported.

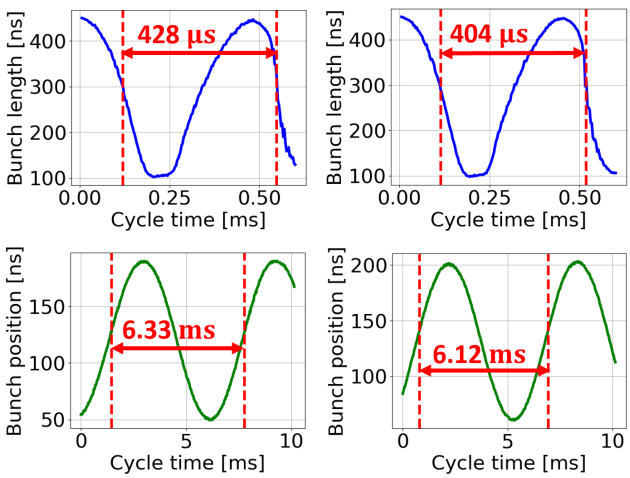

Figure 5: Top: examples of bunch-length evolution for two cycles at flat-bottom with V_p = 5 kV. Left: S13 measured in ring 4. Right: S7 measured in ring 1. Bottom: examples of bunch-position evolution for two cycles at flat-top with V_p = 4 kV. Left: S13 measured in ring 1. Right: S7 measured in ring 3. The bunch lengths are derived by computing the FWHM of the measured bunch profiles, the bunch positions correspond to the central points of the FWHM. For each plot, the vertical lines determine half (top) or one (bottom) synchrotron period, whose values are given as numbers.

second cycle was measured in ring 3 with the S7 cavity, giving V_d = 3.60 kV. The $f_{s,0}$ ratios using detected voltages and synchrotron periods were 1.05 and 1.03, respectively, showing a good agreement (within 2%) between the two methods.

BENCHMARKS WITH SIMULATED DATA

Beam-dynamics simulations including collective effects and using realistic initial bunch distributions were performed

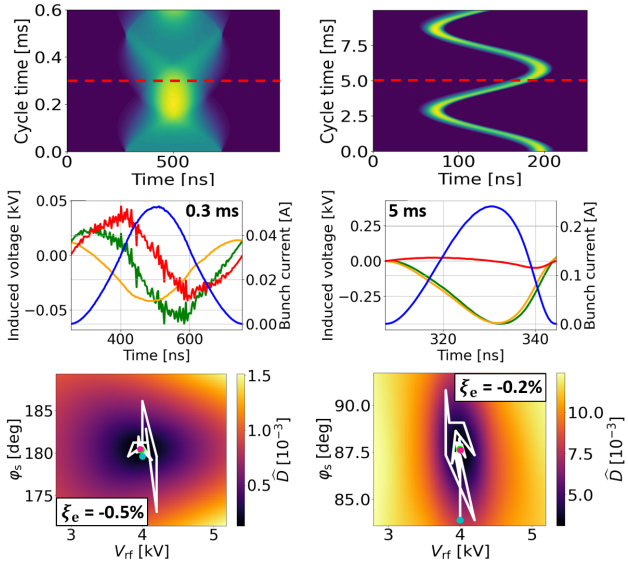

Figure 6: Left, from top to bottom: simulated profiles at injection energy, profile (blue) at 0.3 ms with space charge (red), impedance (orange) and total (green) induced voltages, voltage calibration. Right: corresponding plots for simulated profiles at extraction energy.

with the CERN BLonD code [9]. The goal was to verify that voltage calibrations using the simulated profiles provided as result the RF voltage (4 kV) assumed in simulations.

At flat-bottom, the bunch intensity was $N_p = 8 \cdot 10^{10}$ p/b and the space charge was modelled as an inductive impedance with $|Z/n| = 640\ \Omega$ [10]. The voltage calibration provided a voltage error of just −0.5% (Fig. 6, left).

At flat-top, the induced voltage was dominated by the resistive impedance of the RF cavities, the space charge voltage ($|Z/n| = 17\ \Omega$) became almost negligible. Figure 6 (right) shows that ξ_e was only -0.2%. The voltage difference was just 7 V, much lower than the peak induced voltage of 500 V during bunch oscillations: the induced voltage was mostly resistive, so the bunch synchrotron frequency, and therefore V_d, was only slightly affected by collective effects.

CONCLUSIONS

Tomography-based voltage calibrations were systematically applied in the PSB. The measured time-spans were in general sufficient to obtain convergence in voltage errors, which arrived up to 20%. The spreads from cycle to cycle were negligible. The spreads due to different programmed voltages and beam energies were small. Since the transfer function for the gap return has approximately constant gain over the considered frequency range and is independent of signal amplitude, this was expected.

Synchrotron frequency ratios were computed using detected voltages and synchrotron periods. The agreements were good, demonstrating the consistency of the voltage-calibration results. Benchmarks with realistic simulated profiles provided voltage errors below 1%, indicating that

ISBN: 978-3-95450-227-1 ISSN: 2673-5490 doi:10.18429/JACoW-IPAC2022-TUPOST006

the voltage calibrations applied to the measured profiles are reliable.

REFERENCES

[1] S. Hancock, "A simple algorithm for longitudinal phase space tomography," Tech. Rep. CERN, Geneva, Switzerland, CERN-PS-RF-NOTE-97-06, 1997.

[2] S. Hancock and J.-L. Sanchez Alvarez, "A pedestrian guide to online phase space tomography in the CERN complex," Tech. Rep. CERN-PS-RF-NOTE-2001-010, Geneva, Switzerland, 2001.

[3] S. Hancock, "The development of longitudinal phase space tomography in the PS," in *Fifty years of the CERN Proton Synchrotron*, Geneva, Switzerland, 2011, pp. 155–159.

[4] S. C. P. Albright, A. Lasheen, A. H. C. Lu, and C. H. Grindheim, "Recent Developments in Longitudinal Phase Space Tomography," Bangkok, Thailand, Jun. 2022, presented at IPAC'22, Bangkok, Thailand, Jun. 2022, paper MOPOPT043, this conference.

[5] S. Hancock, M. Angoletta, and A. Findlay, "LEIR RF voltage calibration using phase space tomography," Tech. Rep. CERN, Geneva, Switzerland, CERN-ATS-Note-2010-055 MD, 2010.

[6] D. Quartullo, S. C. P. Albright, H. Damerau, A. Lasheen, G. Papotti, and C. Zisou, "RF Voltage Calibration Using Phase Space Tomography in the CERN SPS," Bangkok, Thailand, Jun. 2022, presented at IPAC'22, Bangkok, Thailand, Jun. 2022, paper TUPOST005, this conference.

[7] H. Damerau *et al.*, "Evaluation of the broadband longitudinal impedance of the CERN PS," Tech. Rep. CERN, Geneva, Switzerland, CERN-ATS-Note-2012-064 MD, 2012.

[8] M. M. Paoluzzi *et al.*, "Design of the New Wideband RF System for the CERN PS Booster," in *Proc. IPAC'16*, Busan, Korea, May 2016, pp. 441–443, doi:10.18429/JACoW-IPAC2016-MOPMW024

[9] CERN Beam Longitudinal Dynamics code BLonD, http://blond.web.cern.ch/.

[10] D. Quartullo, "Simulations of RF beam manipulations including intensity effects for CERN PSB and SPS upgrades," Ph.D. dissertation, Rome Sapienza University, Rome INFN and CERN, 2019, https://cds.cern.ch/record/2658075